CrossMark

TECHNICAL ARTICLE

Crystal structure of fingolimod hydrochloride, $C_{19}H_{34}ClNO_2$

James A. Kaduk,[1,a] Kai Zhong,[2] Amy M. Gindhart,[2] and Thomas N. Blanton
[1]*Illinois Institute of Technology, 3101 S. Dearborn St., Chicago, Illinois 60616*
[2]*ICDD, 12 Campus Blvd., Newtown Square, Pennsylnia 19073-3273*

(Received 10 January 2015; accepted 1 April 2015)

The crystal structure of fingolimod hydrochloride ($C_{19}H_{34}ClNO_2$) has been solved and refined using synchrotron X-ray powder diffraction data, and optimized using density functional techniques. Fingolimod hydrochloride crystallizes in space group $P2_1/n$ (#14) with $a = 7.137\,53(5)$, $b = 5.957\,98(4)$, $c = 49.5196(4)$ Å, $\beta = 91.0808(7)°$, $V = 2105.46(2)$ Å^3, and $Z = 4$. The structure consists of a "lipid bilayer" packing. The polar ends of the molecules make O–H···Cl and N–H···Cl hydrogen bonds to the chloride anion, and the octyl side chains pack adjacent to each other. The hydrogen bonds form three types of chains with graph sets C1,2(7), C1,2(7), and C1,2(8). The result is a complex chain of hydrogen bonds parallel to the *b*-axis. The powder pattern has been submitted to ICDD for inclusion in future releases of the Powder Diffraction File™. © *2015 International Centre for Diffraction Data*. [doi:10.1017/S0885715615000317]

Key words: fingolimod, Gilenya, powder diffraction, Rietveld refinement, density functional theory

I. INTRODUCTION

Fingolimod hydrochloride (marketed as Gilenya®) is an immunomodulatory drug used for the treatment of multiple sclerosis. It works as a sphingosine-1-phosphate receptor modulator, which sequesters lymphocytes in lymph nodes, preventing them from contributing to an autoimmune reaction (Billich *et al.*, 2003). The systematic name (CAS registry number 162359-56-0) is 2-amino-2-[2-(4-octylphenyl)ethyl] propane-1,3-diol hydrochloride. A two-dimensional molecular diagram of the cation is shown in Figure 1.

The presence of high-quality reference powder patterns in the powder diffraction file (PDF; ICDD, 2014) is important for phase identification, particularly by pharmaceutical, forensic, and law enforcement scientists. The crystal structures of a significant fraction of the largest dollar volume pharmaceuticals have not been published, and thus calculated powder patterns are not present in the PDF-4 databases. Sometimes experimental patterns are reported, but they are generally of low quality. This structure is a result of a collaboration among ICDD, Illinois Institute of Technology (IIT), Poly Crystallography Inc., and Argonne National Laboratory to measure high-quality synchrotron powder patterns of commercial pharmaceutical ingredients, include these reference patterns in the PDF, and determine the crystal structures of these active pharmaceutical ingredients (APIs).

Even when the crystal structure of an API is reported, the single-crystal structure was often determined at low temperature. Most powder measurements are performed at ambient conditions. Thermal expansion (often anisotropic) means that the peak positions calculated from a low-temperature single-crystal structure often differ significantly from those measured at ambient conditions. These peak shifts can result in failure of default search/match algorithms to identify a phase, even when it is present in the sample. High-quality reference patterns measured at ambient conditions are thus critical for easy identification of APIs using standard powder diffraction practices.

II. EXPERIMENTAL

Fingolimod hydrochloride was commercial reagent, purchased from AbMole BioScience, and was used as-received. The white powder was packed into a 1.5 mm diameter Kapton capillary, and rotated during the measurement at ~50 cycles s^{-1}. The powder pattern was measured at 295 K at beam line 11-BM (Lee *et al.*, 2008; Wang *et al.*, 2008) of the Advanced Photon Source at Argonne National Laboratory using a wavelength of 0.413 906 Å from 0.5° to 50°2θ with a step size of 0.001° and a counting time of 0.1 s step^{-1}. The pattern was indexed on a primitive monoclinic unit cell having $a = 7.1414$, $b = 5.9600$, $c = 49.5275$ Å, $\beta = 91.046$, $V = 2106.69$ Å^3, and $Z = 4$ using DICVOL06 (Louër and Boultif, 2007). The space group was indicated to be $P2_1/n$ by EXPO2013 (Altomare *et al.*, 2013). A reduced cell search in the Cambridge Structural Database (Allen, 2002) yielded 11 hits, but no crystal structure for fingolimod hydrochloride.

A fingolimod molecule was built and its conformation optimized using Spartan '14 (Wavefunction, 2013), and saved as a mol2 file. This file was converted into a Fenske–Hall *Z*-matrix file using OpenBabel (O'Boyle *et al.*, 2011). This

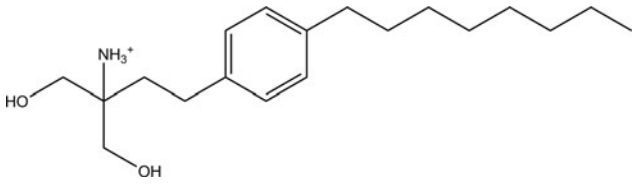


Figure 1. The molecular structure of the fingolimod cation.

[a]Author to whom correspondence should be addressed. Electronic mail: kaduk@polycrystallography.com

https://doi.org/10.1017/S0885715615000317 Published online by Cambridge University Press

molecule and a chlorine atom were used as fragments to solve the structure using FOX (Favre-Nicolin and Černý, 2002). Positions of the active hydrogens were deduced by an analysis of potential hydrogen bonding.

Rietveld refinement was carried out using GSAS (Larson and Von Dreele, 2004). Only the 0.8°–20° portion of the pattern was included in the refinement, and the region 1.3°–1.8° (which contained an unindexed impurity peak of ~2% relative intensity) was excluded. The C22-H31 C_6H_4 phenyl ring was refined as a rigid body. All other non-hydrogen bond distances and angles were subjected to restraints, based on a Mercury/Mogul Geometry Check (Bruno *et al.*, 2004; Sykes *et al.*, 2011) of the molecule. The Mogul average and standard deviation for each quantity were used as the restraint parameters. The restraints contributed 0.92% to the final χ^2. Isotropic displacement coefficients were refined, grouped by chemical similarity. The hydrogen atoms were included in calculated positions, which were recalculated during the refinement. The U_{iso} of each hydrogen atom was constrained to be 1.3× that of the heavy atom to which it is attached. The peak profiles were described using profile function #4 (Finger *et al.* 1994; Thompson *et al.* 1987), which includes the Stephens (1999) anisotropic strain broadening model. Unusually, the S/L profile term was refined to obtain the best fit; it refined to a value of 0.002 249(7), compared with the instrument value of 0.0011. The background was modeled using a three-term shifted Chebyshev polynomial and a six-term diffuse scattering (Debye) function, to model the scattering from the Kapton capillary and any amorphous component of the sample. Given the expected platy morphology of the crystals, a 4th-order spherical harmonic preferred orientation correction was included in the model. The final refinement of 96 variables using 18 736 observations (18 699 data points and 37 restraints) yielded the residuals $R_{wp} = 0.0697$, $R_p = 0.0569$, and $\chi^2 = 1.166$. The largest peak (1.30 Å from N12) and hole (1.55 Å from C1) in the difference Fourier map were 0.24 and −0.19 e (Å^{-3}), respectively. The Rietveld plot is included as Figure 2. The largest errors are in the shapes of some of the low-angle peaks, which may indicate subtle changes in the specimen during the measurement.

A density functional geometry optimization (fixed experimental unit cell) was carried out using CRYSTAL09 (Dovesi et al., 2005). The basis sets for the H, C, N, and O atoms were those of Gatti *et al.* (1994), and the basis set for Cl was that of Apra *et al.* (1993). The calculation used 8 k-points and the B3LYP functional.

III. RESULTS AND DISCUSSION

The refined atom coordinates of fingolimod hydrochloride are reported in Table I, and the coordinates from the density functional theory (DFT) optimization in Table II. The U_{iso} of the atoms in the octyl side chain are not especially large, providing no indication of disorder of the side chain. The root-mean-square deviation of the non-hydrogen atoms is 0.60 Å, and the maximum deviation is 1.97 Å, at O8 (Figure 3). The differences indicate difficulty in refining the conformation of the octyl side chain. Most notable is the difference between the orientation of the hydroxyl group O8–H9 in the refined and optimized structures. Re-starting the refinement from the DFT-optimized structure leads to the same refined model reported here. We believe that the DFT structure is correct, as it results in a more chemically reasonable hydrogen-bonding pattern, but report both structures here so that the reader can choose his/her preferred one. The discussion of the geometry uses the DFT-optimized structure. The asymmetric unit (with atom numbering) is illustrated in Figure 4, and the crystal structure is presented in Figure 5.

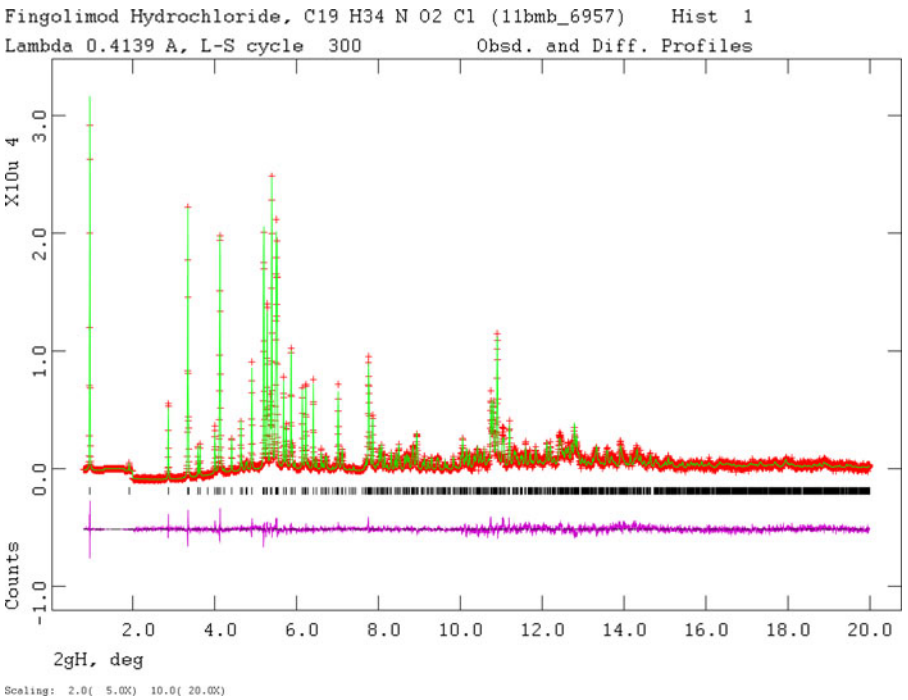


Figure 2. (Color online) The Rietveld plot for the refinement of fingolimod hydrochloride. The red crosses represent the observed data points, and the green line is the calculated pattern. The magenta curve is the difference pattern, plotted at the same vertical scales as the other patterns. The vertical scale has been multiplied by a factor of 5 for $2\theta > 2.0°$, and by a factor of 20 for $2\theta > 10.0°$. The 1.3°–1.8° excluded region (which contains the impurity peak) is not included.

https://doi.org/10.1017/S0885715615000317 Published online by Cambridge University Press

TABLE I. Rietveld refined crystal structure of fingolimod hydrochloride.

Crystal data	
$C_{19}H_{34}ClNO_2$	$\beta = 91.0808\ (7)°$
$M_r = 343.94$	$V = 2105.46\ (2)$ Å^3
Monoclinic, $P2_1/n$	$Z = 4$
$a = 7.137\ 53\ (5)$ Å	Synchrotron radiation, $\lambda = 0.413\ 906$ Å
$b = 5.957\ 98\ (4)$ Å	$T = 295$ K
$c = 49.5196\ (4)$ Å	Cylinder, 1.5 × 1.5 mm
Data collection	
11-BM APS diffractometer	Scan method: step
Specimen mounting: Kapton capillary	$2\theta_{min} = 0.5°$, $2\theta_{max} = 50°$, $2\theta_{step} = 0.001°$
Data collection mode: transmission	
Refinement	
Least-squares matrix: full	18 699 data points
$R_p = 0.057$	97 parameters
$R_{wp} = 0.070$	37 restraints
$R_{exp} = 0.065$	$(\Delta/\sigma)_{max} = 0.05$
$\chi^2 = 1.166$	

Fractional atomic coordinates and isotropic displacement parameters (Å^2)

	x	y	z	U_{iso}
C1	0.7943 (10)	0.0678 (10)	0.783 92 (16)	0.063 (3)
C2	0.9590 (8)	0.2227 (10)	0.791 91 (12)	0.063 (3)
C3	1.1170 (10)	0.0823 (10)	0.804 77 (14)	0.063 (3)
H4	0.703 36	0.025 39	0.802 94	0.082 (3)
H5	0.843 32	−0.107 77	0.776 06	0.082 (3)
H6	1.048 13	−0.022 18	0.822 11	0.082 (3)
H7	1.222 01	0.198 52	0.813 16	0.082 (3)
O8	0.6698 (7)	0.1639 (8)	0.764 88 (13)	0.0662 (15)
H9	0.589 57	0.295 67	0.772 78	0.086 (2)
O10	1.1750 (7)	−0.0695 (8)	0.784 60 (12)	0.0662 (15)
H11	1.334 77	−0.052 88	0.786 06	0.086 (2)
N12	1.0273 (9)	0.3189 (10)	0.766 06 (14)	0.0662 (15)
H13	1.094 81	0.177 13	0.753 99	0.086 (2)
H14	1.124 98	0.454 18	0.7709	0.086 (2)
H15	0.601 74	−0.1175	0.746 16	0.086 (2)
C16	0.9120 (10)	0.4267 (10)	0.809 79 (15)	0.077 (3)
C17	0.8560 (11)	0.3693 (11)	0.838 45 (16)	0.077 (3)
H18	0.802 79	0.531 53	0.797 98	0.101 (4)
H19	1.046 29	0.527 79	0.8116	0.101 (4)
H20	0.952 84	0.257 98	0.847 95	0.101 (4)
H21	0.707 11	0.265 14	0.835 19	0.101 (4)
C22	0.8016 (8)	0.5772 (6)	0.854 59 (10)	0.094 (2)
C23	0.9341 (5)	0.6886 (9)	0.870 62 (12)	0.094 (2)
C24	0.8804 (7)	0.8693 (9)	0.886 53 (9)	0.094 (2)
C25	0.6941 (8)	0.9385 (7)	0.886 40 (9)	0.094 (2)
C26	0.5616 (5)	0.8270 (9)	0.870 37 (12)	0.094 (2)
C27	0.6153 (7)	0.6464 (8)	0.854 47 (9)	0.094 (2)
H28	1.0626 (5)	0.6409 (14)	0.870 70 (18)	0.122 (3)
H29	0.9718 (10)	0.9461 (13)	0.897 58 (13)	0.122 (3)
H30	0.4331 (5)	0.8747 (13)	0.870 29 (18)	0.122 (3)
H31	0.5239 (10)	0.5695 (12)	0.843 41 (13)	0.122 (3)
C32	0.6431 (9)	1.1315 (11)	0.904 02 (18)	0.0992 (16)
C33	0.4333 (9)	1.1653 (12)	0.9094 (2)	0.0992 (16)
C34	0.3976 (9)	1.3626 (13)	0.928 83 (19)	0.0992 (16)
C35	0.1849 (9)	1.3735 (11)	0.933 63 (17)	0.0992 (16)
C36	0.1399 (9)	1.5791 (11)	0.951 08 (18)	0.0992 (16)
C37	−0.0697 (9)	1.5804 (11)	0.957 36 (18)	0.0992 (16)
C38	−0.1046 (8)	1.7945 (12)	0.9742 (2)	0.0992 (16)
C39	−0.3137 (9)	1.8209 (11)	0.9810 (2)	0.0992 (16)
H40	0.673 74	1.295 98	0.892 49	0.129 (2)
H41	0.723 04	1.130 64	0.923 41	0.129 (2)
H42	0.398 38	0.988 77	0.924 59	0.129 (2)
H43	0.340 14	1.130 41	0.891 97	0.129 (2)
H44	0.418 47	1.510 87	0.912 96	0.129 (2)
H45	0.486 36	1.370 12	0.945 35	0.129 (2)
H46	0.155 11	1.201 08	0.947 54	0.129 (2)
H47	0.090 78	1.347 33	0.915 42	0.129 (2)
H48	0.176 45	1.724 52	0.938 01	0.129 (2)
H49	0.227 62	1.571 82	0.970 14	0.129 (2)
H50	−0.105 54	1.422 17	0.970 01	0.129 (2)
H51	−0.155 33	1.570 56	0.937 49	0.129 (2)
H52	−0.078 77	1.9457	0.959 72	0.129 (2)
H53	−0.011 12	1.798 95	0.991 77	0.129 (2)
H54	−0.353 12	1.609 31	0.987 67	0.129 (2)
H55	−0.406 56	1.833 26	0.962 48	0.129 (2)
H56	−0.341 35	1.909 84	0.997 85	0.129 (2)
Cl57	1.0793 (3)	0.0263 (4)	0.711 48 (6)	0.0533 (11)

The powder pattern of the form characterized here appears to correspond to that of form α (the room temperature polymorph) claimed in the US Patent 2013/0281739 A1 (Shrawat *et al.*, 2013). The patterns of forms β and μ differ significantly.

All bond distances and angles, and most torsion angles fall within the normal ranges indicated by a Mercury Mogul Geometry Check. The torsion angles O10–C3–C2–C16, C24–C25–C32–C33, C26–C25–C32–C33, and C36–C35–C34–C33 are flagged as unusual, but they lie on the tails of the normal distributions of these torsion angles. The hydrogen bonds certainly contribute to the orientation of the hydroxyl groups.

Conformational analysis of the fingolimod cation (Hartree–Fock/3-21G/water) using Spartan '14 suggests that the solid state conformation is at least 24 kcal mol^{-1} higher in energy than the minimum-energy conformation. The differences lie mainly in the orientations of the phenyl ring and the polar end of the molecule. Apparently hydrogen bonding is important in determining the solid state conformation. An analysis of the contributions to the total crystal energy using the Forcite module of Materials Studio (Accelrys, 2013) suggests that bond, angle, and torsion distortion terms contribute little to the crystal energy. The energy appears to be dominated by van der Waals and electrostatic contributions, which in this force-field-based analysis include hydrogen bonds. The hydrogen bonds are better analyzed using the results of the DFT calculation.

The structure consists of a "lipid bilayer" packing. The polar ends of the molecules make O–H···Cl and N–H···Cl hydrogen bonds (Table III) to the chloride anion, and the octyl side chains pack adjacent to each other. The hydrogen bonds form three types of chains with graph sets (Etter, 1990; Bernstein *et al.*, 1995; Shields *et al.*, 2000) C1,2(7), C1,2(7), and C1,2(8). The result is a complex chain of hydrogen bonds parallel to the *b*-axis. The ammonium hydrogen H15 does not participate in hydrogen bonds.

The Bravais–Friedel–Donnay–Harker (Bravais, 1866; Friedel, 1907; Donnay and Harker, 1937) morphology suggests that we might expect platy morphology for fingolimod hydrochloride, with {001} as the principal faces. A fourth-order spherical harmonic preferred orientation model was included in the refinement; the texture index was 1.083, indicating that preferred orientation was significant even for this rotated capillary specimen. The powder pattern of fingolimod hydrochloride has been submitted to ICDD for inclusion in future releases of the PDF.

https://doi.org/10.1017/S0885715615000317 Published online by Cambridge University Press

TABLE II. Density functional theory optimized (CRYSTAL09) crystal structure of fingolimod hydrocloride.

Crystal data

$C_{19}H_{34}ClNO_2$
$M_r = 343.94$
Monoclinic, $P2_1/n$
$a = 7.1389$ Å
$b = 5.9574$ Å
$c = 49.5492$ Å
$\beta = 91.0769°$
$V = 2106.93$ Å^3
$Z = 4$

Fractional atomic coordinates and isotropic displacement parameters (Å^2)

	x	y	z	U_{iso}
C1	0.888 39	0.182 68	0.784 68	0.056 40
C2	1.035 60	0.360 42	0.793 47	0.056 40
C3	1.217 70	0.252 91	0.804 40	0.056 40
H4	0.771 21	0.266 91	0.774 16	0.073 40
H5	0.832 72	0.108 83	0.803 07	0.073 40
H6	1.291 84	0.374 76	0.816 39	0.073 40
H7	1.181 56	0.106 85	0.816 74	0.073 40
O8	0.959 13	0.001 87	0.769 15	0.054 00
H9	0.963 81	0.050 47	0.750 39	0.070 20
O10	1.331 25	0.193 57	0.782 47	0.054 00
H11	1.411 21	0.068 50	0.787 99	0.070 20
N12	1.089 97	0.503 42	0.769 38	0.054 00
H13	1.085 63	0.414 35	0.751 51	0.070 20
H14	1.224 96	0.564 85	0.772 09	0.070 20
H15	1.005 97	0.643 49	0.767 40	0.070 20
C16	0.953 47	0.529 51	0.813 48	0.042 70
C17	0.919 39	0.446 66	0.842 29	0.042 70
H18	0.821 55	0.595 31	0.805 03	0.055 50
H19	1.050 84	0.671 75	0.814 76	0.055 50
H20	1.048 24	0.376 30	0.851 18	0.055 50
H21	0.814 80	0.312 48	0.842 47	0.055 50
C22	0.855 05	0.642 06	0.859 23	0.078 50
C23	0.985 43	0.776 89	0.873 13	0.078 50
C24	0.927 51	0.959 31	0.888 38	0.078 50
C25	0.737 20	1.014 20	0.890 47	0.078 50
C26	0.608 00	0.884 83	0.875 64	0.078 50
C27	0.666 08	0.702 30	0.860 20	0.078 50
H28	1.133 63	0.736 37	0.872 20	0.102 10
H29	1.030 82	1.059 24	0.899 42	0.102 10
H30	0.459 80	0.924 49	0.876 09	0.102 10
H31	0.563 67	0.606 66	0.848 48	0.102 10
C32	0.682 19	1.201 32	0.909 47	0.086 70
C33	0.480 63	1.287 80	0.907 49	0.086 70
C34	0.431 67	1.432 75	0.931 86	0.086 70
C35	0.242 51	1.553 49	0.928 96	0.086 70
C36	0.152 94	1.599 66	0.956 20	0.086 70
C37	−0.020 61	1.750 68	0.955 06	0.086 70
C38	−0.123 95	1.752 56	0.981 84	0.086 70
C39	−0.292 51	1.910 05	0.982 45	0.086 70
H40	0.709 58	1.143 15	0.930 23	0.112 70
H41	0.777 15	1.343 74	0.906 57	0.112 70
H42	0.381 03	1.147 64	0.906 27	0.112 70
H43	0.462 36	1.384 27	0.888 78	0.112 70
H44	0.542 71	1.557 09	0.935 54	0.112 70
H45	0.431 09	1.325 56	0.949 93	0.112 70
H46	0.145 61	1.450 78	0.916 69	0.112 70
H47	0.259 98	1.710 78	0.917 78	0.112 70
H48	0.257 65	1.673 00	0.970 17	0.112 70
H49	0.114 63	1.437 60	0.965 08	0.112 70
H50	−0.116 67	1.695 49	0.938 82	0.112 70
H51	0.020 80	1.922 63	0.949 81	0.112 70
H52	−0.024 42	1.798 77	0.998 05	0.112 70
H53	−0.169 97	1.581 33	0.986 38	0.112 70
H54	−0.359 57	1.904 84	1.002 10	0.112 70
H55	−0.398 29	1.863 66	0.967 14	0.112 70
H56	−0.252 11	2.084 59	0.978 63	0.112 70
Cl57	1.003 89	0.225 35	0.712 40	0.082 50

https://doi.org/10.1017/S0885715615000317 Published online by Cambridge University Press

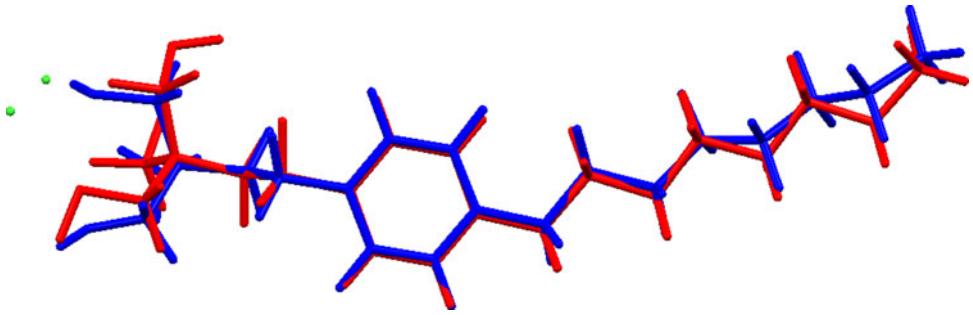


Figure 3. (Color online) Comparison of the GSAS-refined and DFT-optimized structures of fingolimod hydrochloride. The Rietveld-refined structure is colored red, and the DFT-optimized structure is in blue.

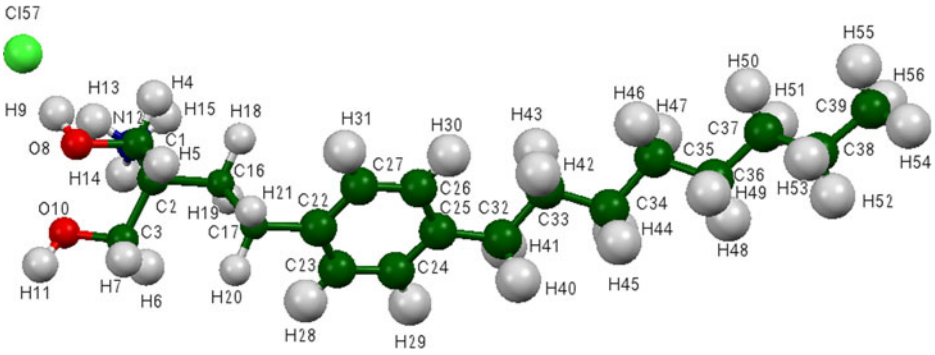


Figure 4. (Color online) The molecular structure of fingolimod hydrochloride, with the atom numbering. The atoms are represented by 50% probability spheroids.

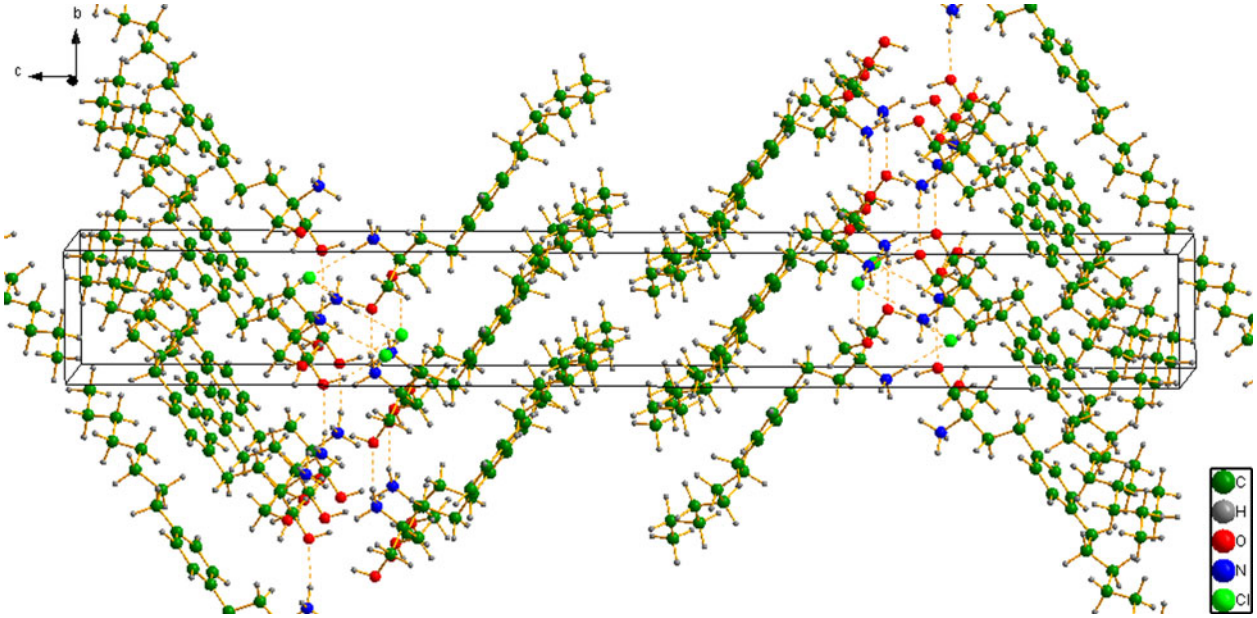


Figure 5. (Color online) The crystal structure of fingolimod hydrochloride, viewed down the *a*-axis.

TABLE III. Hydrogen bonds in fingolimod hydrochloride.

D–H···A	D–H (Å)	H···A (Å)	D···A (Å)	D–H···A(°)	Overlap (*e*)
O8–H9···Cl57	0.975	2.175	3.133	167.2	0.044
O10–H11···Cl57	0.975	2.132	3.036	153.6	0.041
N12–H14···Cl57	1.037	2.279	3.297	166.6	0.049
N12–H13···Cl57	1.032	2.307	3.321	167.0	0.057

https://doi.org/10.1017/S0885715615000317 Published online by Cambridge University Press

ACKNOWLEDGMENTS

Use of the Advanced Photon Source at Argonne National Laboratory was supported by the US Department of Energy, Office of Science, Office of Basic Energy Sciences, under Contract No. DE-AC02-06CH11357. This work was partially supported by the International Centre for Diffraction Data. We thank Lynn Ribaud for his assistance in data collection.

SUPPLEMENTARY MATERIALS AND METHODS

The supplementary material for this article can be found at http://www.journals.cambridge.org/PDJ

Accelrys (**2013**). *Materials Studio 7.0* (Accelrys Software Inc., San Diego, CA).

Allen, F. H. (**2002**). "The Cambridge Structural Database: a quarter of a million crystal structures and rising," Acta Crystallogr. Sect. B: Struct. Sci. **58**, 380–388.

Altomare, A., Cuocci, C., Giacovazzo, C., Moliterni, A., Rizzi, R., Corriero, N., and Falcicchio, A. (**2013**). "EXPO2013: a kit of tools for phasing crystal structures from powder data", J. Appl. Crystallogr. **46**, 1231–1235.

Apra, E., Causa, M., Prencipe, M., Dovesi, R., and Saunders, V. R. (**1993**). "On the structural properties of NaCl: an *ab initio* study of the B1–B2 phase transition," J. Phys., Condens. Matter **5**(18), 2969–2976.

Bernstein, J., Davis, R. E., Shimoni, L., and Chang, N. L. (**1995**). "Patterns in hydrogen bonding: functionality and graph set analysis in crystals," Angew. Chem., Int. Ed. Engl. **34**(15), 1555–1573.

Billich, A., Bornancin, F., Dévay, P., Mechtcheriakova, D., Urtz, N., and Baumruker, T. (**2003**). "Phosphorylation of the immunomodulatory drug FTY720 by sphingosine kinases," J. Biol. Chem. **278**(48), 47408–47415.

Bravais, A. (**1866**). *Etudes Cristallographiques* (Gauthier Villars, Paris).

Bruno, I. J., Cole, J. C., Kessler, M., Luo, J., Motherwell, W. D. S., Purkis, L. H., Smith, B. R., Taylor, R., Cooper, R. I., Harris, S. E., and Orpen, A. G. (**2004**). "Retrieval of crystallographically-derived molecular geometry information," J. Chem. Inf. Sci. **44**, 2133–2144.

Donnay, J. D. H. and Harker, D. (**1937**). "A new law of crystal morphology extending the law of Bravais," Amer. Mineral. **22**, 446–467.

Dovesi, R., Orlando, R., Civalleri, B., Roetti, C., Saunders, V. R., and Zicovich-Wilson, C. M. (**2005**). "CRYSTAL: a computational tool for the *ab initio* study of the electronic properties of crystals," Z. Kristallogr. **220**, 571–573.

Etter, M. C. (**1990**). "Encoding and decoding hydrogen-bond patterns of organic compounds," Acc. Chem. Res. **23**(4), 120–126.

Favre-Nicolin, V. and Černý, R. (**2002**). "FOX, Free Objects for crystallography: a modular approach to ab initio structure determination from powder diffraction," J. Appl. Crystallogr. **35**, 734–743.

Finger, L. W., Cox, D. E., and Jephcoat, A. P. (**1994**). "A correction for powder diffraction peak asymmetry due to axial divergence," J. Appl. Crystallogr. **27**(6), 892–900.

Friedel, G. (**1907**). "Etudes sur la loi de Bravais," Bull. Soc. Fr. Mineral. **30**, 326–455.

Gatti, C., Saunders, V. R., and Roetti, C. (**1994**). "Crystal-field effects on the topological properties of the electron-density in molecular crystals - the case of urea," J. Chem. Phys. **101**, 10686–10696.

ICDD (**2014**). PDF-4+ 2014 (Database), edited by Dr. Soorya Kabekkodu, Int. Centre for Diffraction Data, Newtown Square, PA, USA.

Larson, A. C. and Von Dreele, R. B. (**2004**). *General Structure Analysis System, (GSAS)* (Los Alamos National Laboratory Report LAUR 86-784).

Lee, P. L., Shu, D., Ramanathan, M., Preissner, C., Wang, J., Beno, M. A., Von Dreele, R. B., Ribaud, L., Kurtz, C., Antao, S. M., Jiao, X., and Toby, B. H. (**2008**). "A twelve-analyzer detector system for high-resolution powder diffraction," J. Synchroton Radiat. **15**(5), 427–432.

Louër, D. and Boultif, A. (**2007**). "Powder pattern indexing and the dichotomy algorithm," Z. Kristallogr. S26, 191–196.

O'Boyle, N., Banck, M., James, C. A., Morley, C., Vandermeersch, T and Hutchison, G. R. (**2011**). "Open Babel: an open chemical toolbox," J. Chem. Inf. **3**, 33.

Shields, G. P., Raithby, P. R., Allen, F. H., and Motherwell, W. S. (**2000**). "The assignment and validation of metal oxidation states in the Cambridge Structural Database," Acta Crystallogr. Sec. B: Struct. Sci. **56**(3), 455–465.

Shrawat, V. K., Veereshappa, N., Singh, V. K., and Purohit, P. (**2013**). "Fingolimod polymorphs and their processes," US Patent 2013/0281739 A1.

Stephens, P. W. (**1999**). "Phenomenological model of anisotropic peak broadening in powder diffraction," J. Appl. Crystallogr. **32**, 281–289.

Sykes, R. A., McCabe, P., Allen, F. H., Battle, G. M., Bruno, I. J., and Wood, P. A. (**2011**). "New software for statistical analysis of Cambridge Structural Database data," J. Appl. Crystallogr. **44**, 882–886.

Thompson, P., Cox, D. E., and Hastings, J. B. (**1987**). "Rietveld refinement of Debye–Scherrer synchrotron X-ray data from Al_2O_3," J. Appl. Crystallogr. **20**(2), 79–83.

Wang, J., Toby, B. H., Lee, P. L., Ribaud, L., Antao, S. M., Kurtz, C., Ramanathan, M., Von Dreele, R. B., and Beno, M. A. (**2008**). "A dedicated powder diffraction beamline at the Advanced Photon Source: commissioning and early operational results," Rev. Sci. Instrum. **79**, 085105.

Wavefunction, Inc. (**2013**). Spartan '14 Version 1.1.0, Wavefunction Inc., 18401 Von Karman Ave., Suite 370, Irvine CA 92612.

https://doi.org/10.1017/S0885715615000317 Published online by Cambridge University Press